Hindawi
Geofluids
Volume 2018, Article ID 4273450, 10 pages
https://doi.org/10.1155/2018/4273450

Research Article

Visualized Experimental Investigation on the Gas-Water Distribution Characteristics in Intersecting Fractures

Chen Wang[1], **Yujing Jiang**[1], **Richeng Liu**[2] and **Changsheng Wang**[1]

[1]*Graduate School of Engineering, Nagasaki University, Nagasaki 8528521, Japan*
[2]*State Key Laboratory for Geomechanics and Deep Underground Engineering, China University of Mining and Technology, Xuzhou 221116, China*

Correspondence should be addressed to Yujing Jiang; jiang@nagasaki-u.ac.jp

Received 17 December 2017; Revised 9 February 2018; Accepted 15 February 2018; Published 26 March 2018

Academic Editor: Fengshou Zhang

In coal-bed methane recovery, water is generally drained out along with gas. In order to address the influence of different gas-water ratios, fracture intersecting angles, and gas desorption positions on gas and water distributions along fractures and hence understand the two-phase flow behavior in fracture network, an experimental study was conducted on three artificial models with intersecting fractures. The results show that (1) with gas and water injected at different rates, the flow of water and gas is divided into three stages. In the first stage, gas flowed as small bubbles. The transport of gas was stable, which was similar to single-phase laminar flow. The difference in gas injection positions led to totally contrary flow results of water and gas. (2) In the second stage, larger gas bubbles were formed and the interactions between water and gas became serious. The gas-water distribution was dominated by different inertias between water and gas. The difference in gas injection positions did not take much effect on the gas-water distribution. (3) In the third stage, the influence of the inertia difference was still important, but some other factors also influenced the gas-water distribution. The difference in gas injection positions led to different distribution results. (4) The water injection rate has impact on the distribution of the water flow rate in each outlet. In the second stage, when water was injected at small rates, the difference between the cases in which gas was injected from different positions can be neglected. When water injection rates became larger, this difference became obvious. (5) The intersecting angle of the fractures influences the distribution of water and gas. The larger the intersecting angle is, the larger the inertial effect will be. Consequently, the intersecting angle influences the length of the second stage, which is dominated by the inertial effect.

1. Introduction

The gas-water two-phase flow exists in many engineering applications, including coal-bed methane recovery, CO_2 sequestration, geothermal energy development, and contaminant transport in geological rock strata [1–5]. Generally, the coal seams are abounded with water, and the recovery of coal-bed methane experiences a two-phase flow process at the initial stage of exploitation. In the first stage of coal-bed methane drainage, water is drained out from the coal seams, which is a single-phase flow process. With the depletion of pressure of the seam, gas in the absorbed phase begins to desorb from the coal matrix. Due to its small quantity, in the second stage, the gas phase is discontinuous and bubbly flow is formed. In the above-mentioned process, there is a transition from single-phase flow to two-phase flow in the fracture network, and the gas desorption rate varies with respect to time. Consequently, a two-phase flow with different gas-water ratios will be formed. This is why the flow behavior with different gas-water ratios requires to be well understood. By the way, the parameters of the fracture network such as the fracture intersecting angle also have an impact on the flow behavior. As a basis, a study on the fracture intersections is needed to seek understanding the influence of parameters such as the intersecting angle on the flow behavior. In applications of coal-bed methane recovery, by investigating the statistical parameters in the coal seam fracture network and based on the field data such as the water or gas percentage and the pressure depletion curve, the

flowing state can be estimated and the optimal exploitation scheme can be determined.

Existing studies on two-phase flow can be divided into two broad categories, namely, the displacement mechanisms [6] and simultaneous flow of two phases in the fractures or porous media [7, 8]. Conventional theories on the two-phase flow originate from the aspection of porous media based on the concept of relative permeability. Commonly used models of relative permeability of two-phase flow in porous media include the X-model [9], the viscous-coupling model [10], and the Brooks-Corey model [11]. The X-model has been used to simulate reservoir behaviors for its priority in simplicity [12, 13], but its application is limited because it neglects the interaction between different phases. In the viscous-coupling model, the interaction between different phases due to the viscosity difference is included [14]. The Corey model is one of the most commonly used models in porous media [15], in which capillary pressure plays a dominant role.

Even though distinct differences exist between rock pores and rock fractures, such as geometry and connectivity, it has been found that the flow behavior of two-phase fluid through a single fracture can be described by models proposed for porous media. In the gas-water flow experiment in smooth fractures by Diomampo, the results followed the Corey model [16], which indicates that in some cases the two-phase flow behavior in fractures is a limiting case of that in porous media. Romm conducted the kerosene-water two-phase flow tests in parallel artificial fractures, which confirmed to the X-model. Fourar and Bories investigated the air-water flow in parallel artificial fractures, and the relative permeability complies with viscous-coupling model [17]. Watanabe et al. conducted a series of experiments with decane-water and nitrogen-water in real fractures with different wettability values, in which a new v-type relative permeability was indicated [18]. Conventional models for relative permeability are mainly expressed as the function of saturations, which neglects the contributions of fracture roughness. In consideration of this deficiency, Chen established the correlation between the flow structures and the relative permeability in single fractures through visualization experiment [19], in which the flow structures are the indications of fracture roughness and capillary pressure. In addition, the gas-water ratio is a critical and fundamental parameter. Different gas-water ratios will lead to different structures such as bubble flow, slug flow, or stratified flow and correspondingly lead to different influences of viscosity and capillary pressure. Therefore, there will be different pressure drop characteristics [20, 21]. However, the diversity of two-phase models and experimental results in fractures indicates that a more generalized model to describe the multiphase behavior is still absent. Fundamental problems, such as whether the contributions of viscous force or capillary pressure dominate the flow in different kinds of fractures, still require to be investigated.

In addition, most present studies on the two-phase flow in fractures were carried out in a single fracture to achieve their conductivity, while the two-phase flow behavior in combined fractures or fracture network still require to be further investigated. On the distribution characteristics of gas-water two-phase flow, many studies have been conducted in T-junctions [22–25], and the distribution of water and gas is influenced by the effect of inertial effect and gravity [26, 27]. It is reported that gas and water can be separated due to the difference of inertial effects [26, 28–30]. Small bubbles or solid particles are more likely to be carried by the fluid flow, while large bubbles or solid particles are likely to deviate from the streamline of the fluid, and small bubbles or slug bubbles show different inertial effects [31–34]. In a flow channel junction (intersection), different gas-water ratios will lead to different separation results [29] since the influence of the inertial effect is different. Therefore, the gas-water ratio plays a role in two-phase flow behavior which requires to be investigated. Inertia separator is developed based on this mechanism, and, in fractures, it is indicated that the inertial effect cannot be neglected in many conditions [21, 35, 36], so such effects still require to be further studied, especially quantitative investigations are expected. In addition, the flow characteristics in single fractures and fracture intersections provide basis for deeply understanding the fluid flow behavior in the fracture networks. The fractures can intersect at different angles. The intersecting angle is a critical parameter that influences the flow characteristics because the fluid is redistributed at the intersection. Li et al. studied the influence of the intersecting angle on nonlinear flow at fracture intersections. They reported that the larger intersecting angle results in the stronger nonlinearity of flow regimes [37]. In two-phase flow, the phase separation is influenced by the intersecting angle between the two outlets due to the different inertias of the phases [29]. Therefore, the influence of intersecting angle should be investigated.

In the present study, a series of two-phase flow tests were conducted in artificial smooth intersecting fractures with the developed experimental system. Then, the influence of different gas-water ratios, fracture intersecting angles, and gas injection positions on the gas and water distributions was analyzed. This experiment simulates the evolution of water flow rate with respect to different gas desorption rates in coal seams, with the expectation that by evaluating the water flow rate the gas desorption state can also be forecasted. This experiment provides a basis for further studies to understand the distribution of gas and water in the two-phase flow in fracture networks.

2. Experiment

2.1. Experimental Setup. In order to investigate two-phase fluid flow behavior through intersecting fractures, an experimental system was developed. It consists of three main units: the fluids supply unit, the fracture model, and the data measurement unit. The detailed schematic of the experiment system is shown in Figure 1. Gas (Nitrogen) is supplied from the gas cylinder, in which the initial gas pressure is 15 MPa. Since the mass flow controller which was connected to the cylinder cannot bear the pressure over 1 MPa, the pressure is decreased to the range of 0.1–0.3 MPa with a pressure regulator. With the mass flow controller, gas was injected into the testing model with a constant flow rate in a range of 0–2000 mL/min. Gas injection rate can be visually displayed on the digital screen of mass flow controller. Water was

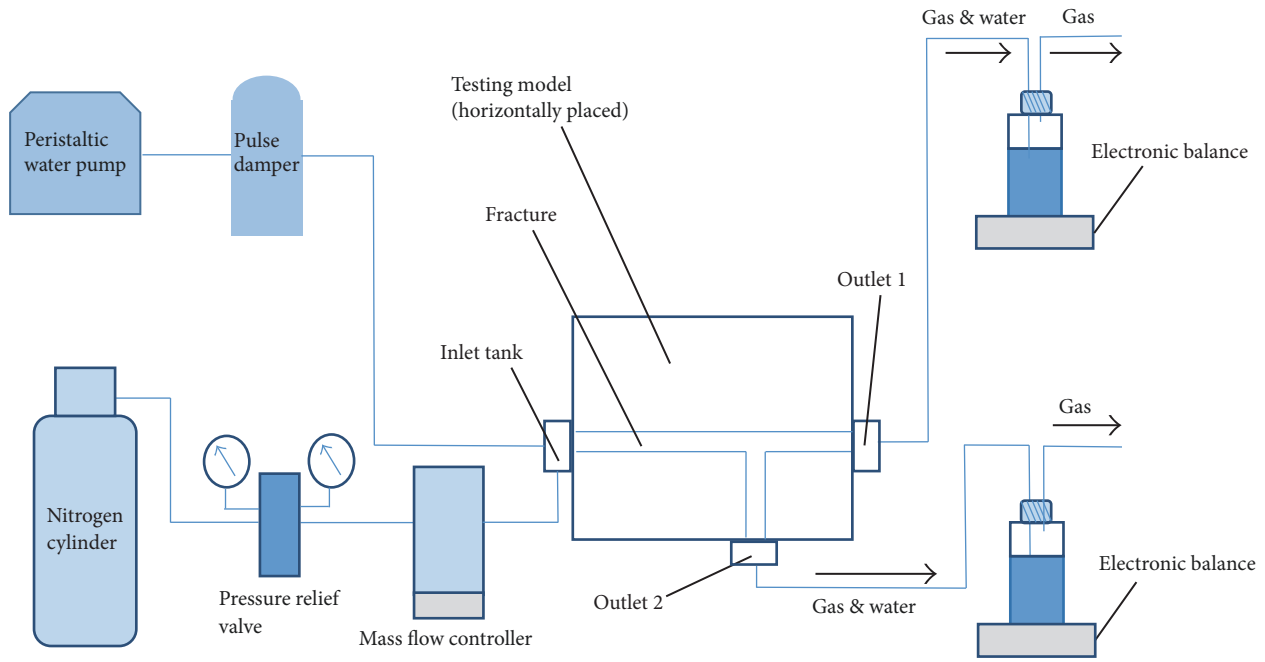

Figure 1: The schematic of the experiment system.

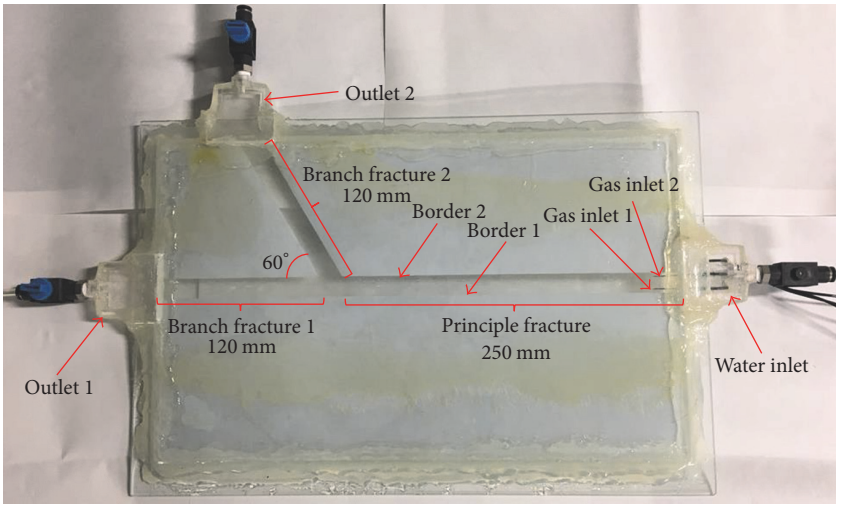

Figure 2: The testing model with fractures intersecting at 60°.

injected with the peristaltic pump with a constant flow rate. In this experiment, water was injected with 500 mL/min, 700 mL/min, 900 mL/min, and 1100 mL/min. Gas and water were injected into the inlet tank of the fracture model simultaneously and flowed out from the two outlet tanks, which are named as Outlet 1 and Outlet 2, respectively. At the two outlets, gas was released to the atmosphere while water was collected in a bottle and weighed by a precise electronic balance. The data of water mass in each bottle was transmitted into the computer in real time. Consequently, the water flow rate was obtained.

Three testing models were manufactured with toughened glasses and resin plates. In each model, two fractures intersect at a certain angle (30°, 60°, or 90°). Figure 2 shows the testing model in which fractures intersect at 60°. Each testing model consists of three layers. Two toughened glasses were used as upper and lower layers, respectively, for purpose of visual observation. Resin plates with a thickness of 1 mm were set as the middle layer. The resin plates have three separate parts to form an artificial fracture with a thickness of 1 mm. The aperture of the fractures is 15 mm. Compared with the aperture of natural fractures, the adopted aperture in the experiment is much larger because we want to visually observe the two-phase flow phenomenon within the void spaces of a fracture. If the fracture aperture is in the natural scale, that is, 0.01~1 mm, it is quite difficult to capture

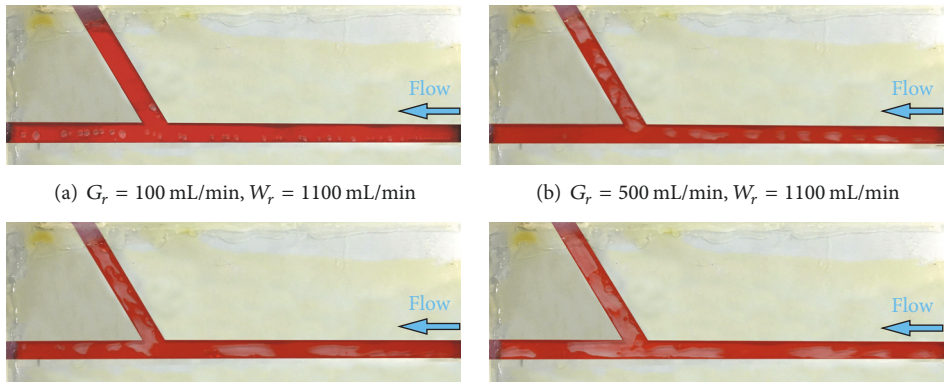

(a) G_r = 100 mL/min, W_r = 1100 mL/min (b) G_r = 500 mL/min, W_r = 1100 mL/min

(c) G_r = 1000 mL/min, W_r = 1100 mL/min (d) G_r = 2000 mL/min, W_r = 1100 mL/min

Figure 3: The flow structures at the water injection rate of 1100 mL/min with gas injected from Gas Inlet 1.

images of fluid flow and bubble distributions using the current visualization techniques. However, we accept that, to simulate the real two-phase flow at the fracture intersection, the fracture that has a real-scale aperture should be used. Therefore, in the following future works, we will investigate the influence of fracture aperture size on the two-phase flow behaviors.

Here we define the principle fracture, Branch Fracture 1, and Branch Fracture 2, as indicated in Figure 2. In each model, both Branch Fracture 1 and Branch Fracture 2 have a length of 120 mm to achieve identical conductivity in two branch fractures. The principle fracture has a length of 250 mm. The only difference between these testing models is the intersecting angle, while all the other sizes are identical. Grease was coated on the resin to restrain the water and gas from flowing into the areas beyond the fractures. At the boundaries of the testing model, silicone sealant was used to fix the glasses and the plate and also for sealing up. Near the water inlet tank, there were two needles with an inner diameter of 0.8 mm acting as gas inlets, as shown in Figure 2. This is designed to estimate the influence of gas injection positions on the water and gas distribution. The two boundaries of the principle fracture are designated as Border 1 and Border 2, respectively.

2.2. The Testing Procedures. If the testing model was not horizontally placed in the test, the two outlets will be of different elevations, and the flow rates of liquids can be seriously influenced. Consequently, prior to the flow test, the testing model was horizontally laid, and the horizontality was checked with a level gauge. In each testing model, Branch Fracture 1 and Branch Fracture 2 have the same fracture thicknesses and widths. Therefore, theoretically they should have identical permeability values when the inertial effects are not strong when fluids transport at small velocity. To further test the horizontality, water was injected to the specimen at very small flow rates. It shows that the flow rates of water from 2 outlets were approximately identical at a flow rate of 30 mm/min, indicating that the specimen was laid flat. Then water was injected to the specimen at a constant flow rate of 500, 700, 900, and 1100 mL/min, and nitrogen was injected with a constant flow rate in the range of 0–2000 mL/min. The gas flow rate of 0–2000 mL/min in this study corresponds to a superficial velocity of 0–2 m/s, and the water flow rate of 500–1100 mL/min corresponds to a superficial velocity of 0.55–1.2 m/s. The gas velocity and flow velocity are in the same order of magnitude as those reported in the literature. For example, to investigate the two-phase flow pressure drop characteristics in fractures, a gas superficial velocity of 0–5 m/s and a water superficial velocity of 0–0.41 m/s were adopted in Fourar and Bories [17]. In each test round, the flow of two different phases of fluid was kept for 1-2 min to achieve a stable flow state prior to the measurement of flow rates in each outlet.

2.3. Results and Discussion. According to the testing results, the distribution of water in the two outlets was seriously influenced when gas was injected at different rates. On the other hand, the water injection rate also had an impact on the distribution of gas in the two outlets. In this study, the evolution of water flow rates in the two outlets was quantitatively measured and analyzed along with the gas flow structures which were qualitatively measured with the visualization photos. The 60° model is firstly selected as an example for analyzing the effect of the gas injection rate.

(1) The Effect of Gas Injection Rate. Figure 3 shows the cases in which water was injected at 1100 mL/min and gas was injected from Gas Inlet 1. The gas injection rate was increased step by step. The evolution of the flow characteristics can be divided into 3 stages.

In the first stage, when gas was injected at a small rate, as shown in Figure 3(a). In this stage, gas bubbles transported in a stable state, and the morphology of gas bubbles was regular. This indicates that the turbulence was not serious, which is similar to the single-phase laminar flow. Since gas was injected from Gas Inlet 1 which is close to Border 1, the gas bubbles flowed along Border 1 of the principle fracture, and consequently almost all the gas transported to Branch Fracture 1. Therefore, more gas was driven to Branch Fracture 2. Corresponding to the transport of gas in this stage, the transport characteristics of water can be indicated in Figure 8.

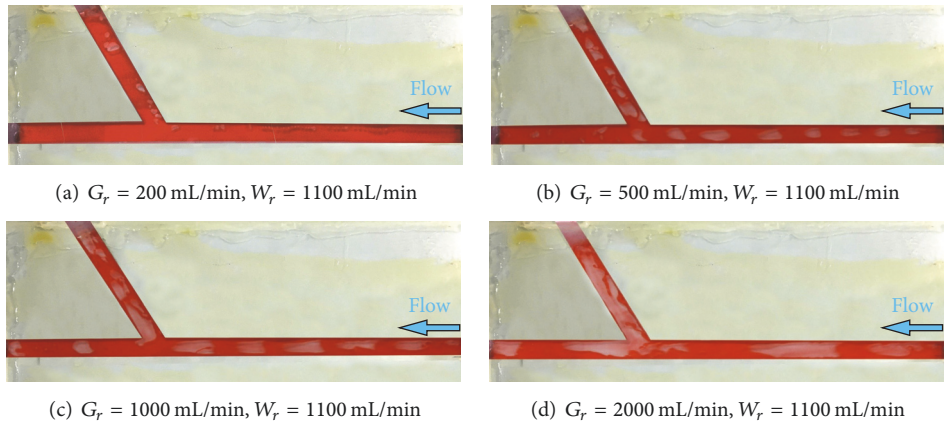

(a) G_r = 200 mL/min, W_r = 1100 mL/min (b) G_r = 500 mL/min, W_r = 1100 mL/min

(c) G_r = 1000 mL/min, W_r = 1100 mL/min (d) G_r = 2000 mL/min, W_r = 1100 mL/min

Figure 4: The flow structures at the water injection rate of 1100 mL/min with gas injected from Gas Inlet 2.

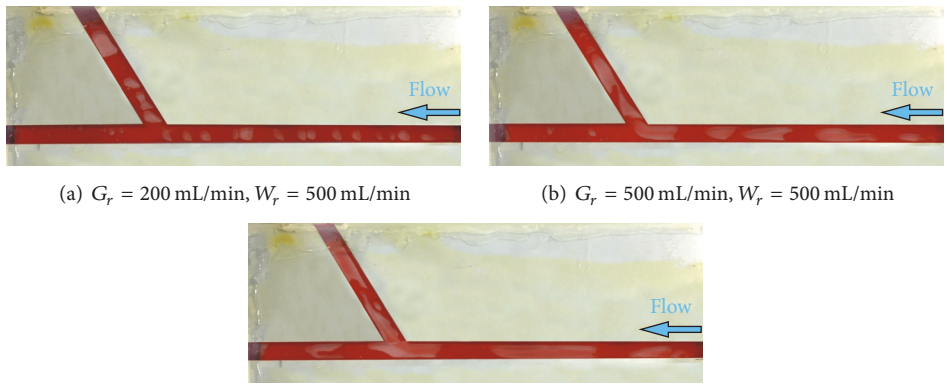

(a) G_r = 200 mL/min, W_r = 500 mL/min (b) G_r = 500 mL/min, W_r = 500 mL/min

(c) G_r = 1000 mL/min, W_r = 500 mL/min

Figure 5: The flow structures at the water injection rate of 500 mL/min with gas injected from Gas Inlet 1.

As shown in Figure 8(a) in which gas was injected from Inlet 1, when water was injected at 500 mL/min (W_r = 500), the water flow rate in Outlet 1 decreased when gas injection rate increased from 0 to 100 mL/min. This is because all the gas bubble transported into Branch Fracture 1 and more water was driven into Branch Fracture 2. This is why the water flow rate in Outlet 2 increased as indicated in Figure 8(b), while the water flow rate in Outlet 1 decreased as indicated in Figure 8(a). When gas was injected from Gas Inlet 2, gas totally flow into Outlet 2, as shown in Figure 4(a); water flow rate in the Outlet 1 increased with respect to the increase of gas injection rate, as shown in Figure 8(a). This is totally contrary to the case when gas was injected from Gas Inlet 1.

To summarize, gas transported stably as small bubbles in this stage. The turbulence was not serious, which was similar to the laminar flow. The difference in gas injection positions would lead to totally contrary flow conditions of both water and gas: when gas was injected from different positions, the gas bubbles flowed into different branch outlets (Figures 3(a) and 4(a)), and the water flow rates in Outlet 1 (Figure 7(a)) would also evolve in opposite trends, as well as that in Outlet 2 (Figure 7(a)).

In the second stage, because gas was injected with a lager rate, larger bubbles were formed, as shown in Figures 3(b) and 4(b). By comparing Figures 3(b) and 4(b), it can be indicated that no matter gas was injected from Gas Inlet 1 or Gas Inlet 2, almost all gas bubbles transported into Branch Outlet 2, which is quite different from the first stage. Comparisons between Figure 5(a) and Figure 6(a) or Figure 5(b) and Figure 6(b) show the same phenomena. Correspondingly, as shown in Figure 8(a), when water flow rate was 500 mL/min, when the gas injection rate was increased 300–900 mL/min, the evolution of water flow rate (with gas injected from Gas Inlet 1) was identical to the evolution of water flow rate (with gas injected from Gas Inlet 2). In Figure 8(b), the same phenomenon is indicated. In this stage larger bubbles were formed, and the morphology of gas bubbles was no longer regular. The turbulence became significant due to the drastic interactions between water and gas, and consequently the gas bubbles no longer remained close to the border. The distribution of water and gas was dominated by the different inertias of water and gas. Both Figures 3(b) and 4(b) show that almost all the gas transported to Branch Fracture 2. In such conditions, the reason why most gas bubbles moved into

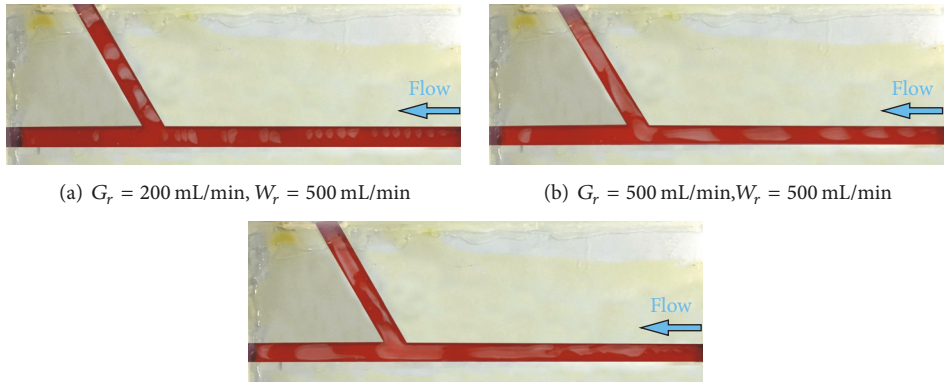

(a) G_r = 200 mL/min, W_r = 500 mL/min

(b) G_r = 500 mL/min,W_r = 500 mL/min

(c) G_r = 1000 mL/min, W_r = 500 mL/min

Figure 6: The flow structures at the water injection rate of 500 mL/min with gas injected from Gas Inlet 2.

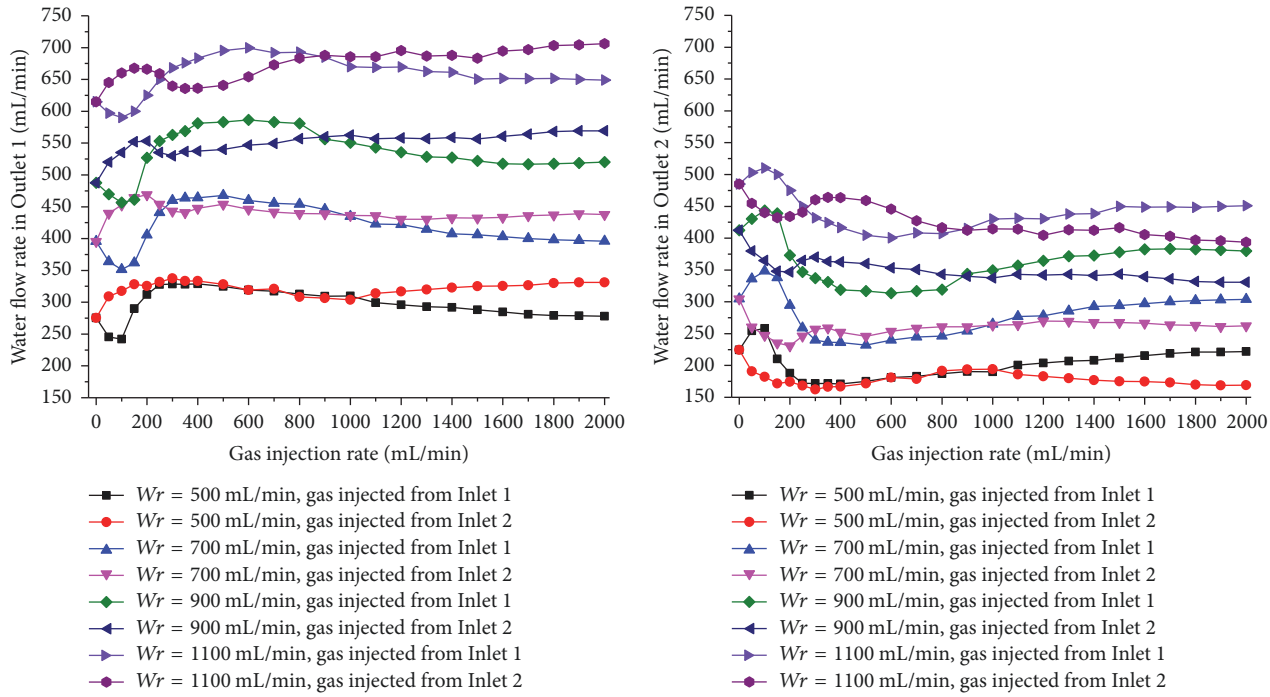

(a) The water flow rate in Outlet 1 in the 30° testing model

(b) The water flow rate in Outlet 2 in the 30° testing model

Figure 7

Branch Outlet 2 is that the density of water is about 800 times as that of gas, and thus there is a difference in the inertial effects. In such conditions, water, the liquid with a larger inertial effect, would be more likely to transport into Branch Outlet 1, which is connected to the principle fracture without diversion angle, and drove gas into Branch Outlet 2.

To summarize, in this stage, the transport of water and gas was quite turbulent with serious interactions between water and gas. The distribution of water and gas was dominated by the different inertias between water and gas, and the gas injection positions did not take much effect on the water and gas distribution when the water flow rate was small.

In the third stage, because gas injection rate was further increased, slug bubbles were formed, as shown in Figures 3(c), 3(d), 4(c), and 4(d). The gas injection rate was larger, and the flow of both water and gas was more turbulent, and there are many factors that influence the distribution of water and gas. The distribution of gas into two outlets became more even, but it is still that more gas transported to Branch Fracture 2, indicating that the effect of different inertias on distribution was still important. Figures 5(c) and 6(c) show the same phenomena. By comparing Figures 3(b), 3(c), and 3(d), it can be noticed that the flow structures evolved from bubble flow to slug flow, and the percentage of gas that transported into Branch Fracture 1 also increased, meaning that the distribution behavior was also influenced by the flow structures. The evolution of the water flow rates in two outlets went into a stable state when gas injection rate

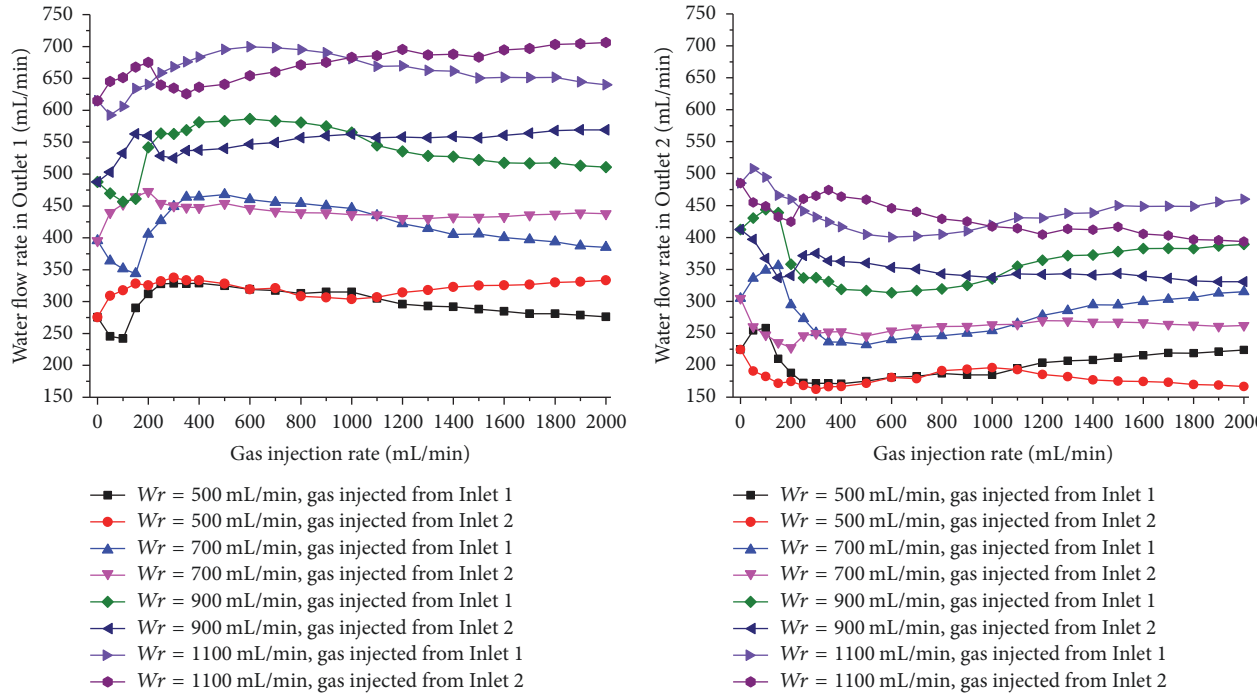

(a) The water flow rate in Outlet 1 in the 60° testing model

(b) The water flow rate in Outlet 2 in the 60° testing model

Figure 8

increased from 1000 to 2000 mL/min, as shown in Figures 8(a) and 8(b). Different from that in the second stage, the difference between the cases in which gas was injected from different positions became obvious. This means that, in this stage, though the effect of different inertias was still important, some other factors also had influence and lead to this difference if gas was injected from different gas injection inlets.

The results of 30° model and 90° model also show the same evolution process, as shown in Figures 7 and 9.

(2) The Effect of Water Injection Rate and Fracture Intersecting Angle. The 90° model is selected as an example for analyzing the effect of water injection rate. Figure 9(a) shows the evolution of water flow rate in Outlet 1 when water was injected with different injection rates at the water inlet, and Figure 9(b) shows that in Outlet 2. As mentioned above, the evolution of gas and water in each outlet can be divided into three stages. It can be indicated in Figures 9(a) and 9(b) that no matter water was injected at which rate (500 mL/min, 700 mL/min, 900 mL/min, and 1100 mL/min), the evolution of the water flow rate in Outlet 1 or Outlet 2 always has these three stages. But at different water injection values, some differences can be noticed. In the second stage, as shown in Figure 9(a), when water was injected at 500 mL/min, the difference between the cases when gas was injected from different positions can be neglected. When water was injected at 700 mL/min, this difference became larger but still not significant. When water was injected at 900 mL and 1100 mL, this difference became obvious. This is because, in the second stage, when water was injected at small rates, such as 500 mL/min, the distribution of water and gas is dominated by the different inertias between water and gas, as mentioned previously. When the water injection rate went higher, the flow became more turbulent and some other factors took more effect which would lead to such a difference. In the third stage, despite the fact that water was injected at different rates, the difference between each case in which gas was injected from different positions was similar.

By comparing Figures 7–9, it can be noticed that, with the increase of intersecting angle, there is some difference in the evolution of water flow rates in the outlets. As mentioned above, the evolution of water flow rates in the two outlets can be divided into three stages. As indicated by Figure 7, for the 30° model, in the cases of W_r = 500 mL/min and W_r = 700 mL/min, when the gas injection rate passed 900 mL/min, the flow of water transferred from the second stage to the third stage. For W_r = 900 mL/min and W_r = 1100 mL/min, this transferring point is 1000 mL/min. For the 60° model, in the cases of W_r = 500 mL/min and W_r = 700 mL/min, this transferring point is 1000 mL/min. For W_r = 900 mL/min and W_r = 1100 mL/min, this transferring point is 1100 mL/min. For the 90° model, in the cases of W_r = 500 mL/min and W_r = 700 mL/min, W_r = 900 mL/min, and W_r = 1100 mL/min, this transferring point is 1200 mL/min. This indicates that, with the increase of the intersecting angle of fractures, the transferring point of the gas injection rate, which indicates the transfer from the second stage to the third stage, would increase. This is because the second stage is dominated by the inertial effect of water and gas. With a

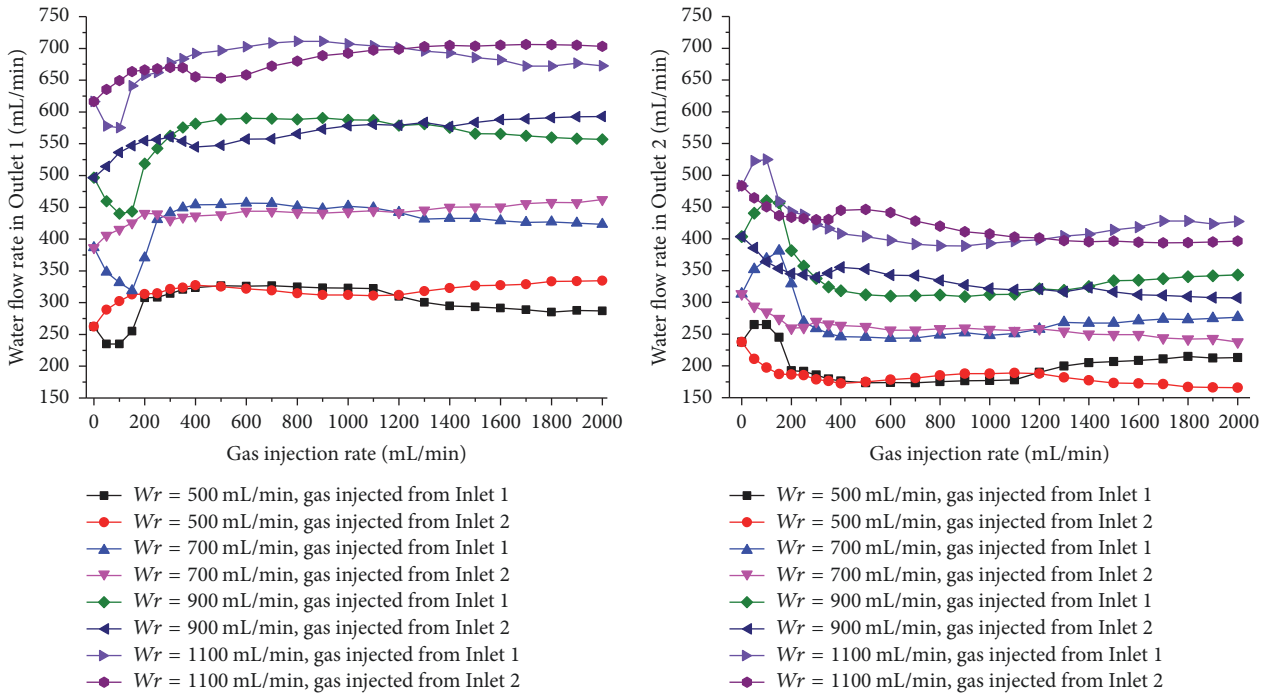

(a) The water flow rate in Outlet 1 in the 90° testing model

(b) The water flow rate in Outlet 2 in the 90° testing model

Figure 9

larger intersecting angle of the two fractures, the difference of the inertial effects between phases will play a more significant role. Consequently, the second stage would be extended in the model with a larger fracture intersecting angle since the second stage is inertial effect dominated.

Actually, the mentioned factors which would influence the distribution of water and gas into two outlets, including the gas injection rate, water injection rate, gas injection positions, and fracture intersecting angle, are coupled with each other, meaning that any variation in one factor will contribute to changes in the magnitudes of the influence by the other factors. It has to be addressed that this study is a preliminary study for the distribution of two flowing phases through two intersecting fractures using the newly developed visualization testing system of two-phase flow. In the present study, the reason why the flow has three stages is that different physical effects take turns to be the dominate factors, so in future studies we will focus on the quantitative analysis of different physical factors including the inertial effect, the viscous effect, the capillary pressure, and so forth to seek more accurate quantitative description methods for describing such flow phenomenon.

3. Conclusions

With the developed visual experimental system, the two-phase flow through different intersecting fractures at different water and gas injection rates is investigated. The results can be concluded as follows.

With gas and water injected at different rates, the flow of both water and gas can be divided into three stages. In the first stage, gas flowed as small bubbles, and the transport of gas and water was stable. The turbulence was not serious, which is similar to the single-phase laminar flow. The difference in gas injection positions would lead to totally contrary flow conditions of both water and gas: when gas was injected from different positions, the gas bubbles flowed into different branch outlets, and the water flow rate in Outlet 1 or Outlet 2 would also evolve in opposite trends.

In the second stage, because larger bubbles were formed, the turbulence became significant due to the drastic interactions between water and gas. The difference of the inertial effects between water and gas dominates the distribution of water and gas. In such conditions, most gas bubbles transported into Branch Outlet 2 and drove more water into Branch Outlet 1. In this stage, the difference in the gas injection positions did not take much effect on the water and gas distribution.

In the third stage, the turbulence became more significant and the interactions between water and gas were more serious. Though the effect of different inertias was still important, some other factors also became to take more effect. The difference of the gas injection positions would lead to different evolution curves of water flow rates in each outlet.

The water injection rate also has impact on the distribution of the water flow rate in each outlet, particularly in the second stage. In the second stage (gas injection rate between 200 and 1000 mL/min), when water was injected in small flow rates (500 mL/min and 700 mL/min), the difference between the cases in which gas was injected from different positions can be neglected. When the water was injected in larger flow rates (900 mL/min and 1100 mL/min), this difference became

obvious. This indicates the transformation from an inertial effect dominated process to a multieffect influenced process. The intersecting angle of the fractures also influences the distribution of water and gas. The larger the intersecting angle is, the larger the inertial effect will be. Consequently, the intersecting angle influences the range of the second stage, which is dominated by the inertial effect.

The factors which influence the distribution of water and gas into two outlets, including the gas injection rate, water injection rate, gas injection positions, and fracture intersecting angle, are coupled with each other, meaning that any variation in one factor will contribute to changes in the influence magnitudes of the other factors, so in future studies more accurate quantitative description methods for such flow phenomenon are supposed to be developed.

Conflicts of Interest

The authors declare that they have no conflicts of interest.

Acknowledgments

This study has been partially funded by JSPS-NSFC Bilateral Joint Research Project, Japan (Grant nos. 17H03506 and 51611140122), the National Natural Science Foundation of China, China (Grant no. 51709260), the Natural Science Foundation of Jiangsu Province, China (no. BK20170276), and China Scholarship Council (CSC). These supports are gratefully acknowledged.

References

[1] S. Kimura, "Geothermal energy development and multiphase flows," *Japanese Journal of Multiphase Flow*, vol. 11, no. 1, pp. 11–14, 1997.

[2] R. L. Detwiler, H. Rajaram, and R. J. Glass, "Interphase mass transfer in variable aperture fractures: Controlling parameters and proposed constitutive relationships," *Water Resources Research*, vol. 45, no. 8, Article ID W08436, 2009.

[3] P. Persoff and K. Pruess, "Two-phase flow visualization and relative permeability measurement in natural rough-walled rock fractures," *Water Resources Research*, vol. 31, no. 5, pp. 1175–1186, 1995.

[4] E. A. Sudicky and E. O. Frind, "Contaminant transport in fractured porous media: Analytical solutions for a system of parallel fractures," *Water Resources Research*, vol. 18, no. 6, pp. 1634–1642, 1982.

[5] P. Nuske, B. Faigle, R. Helmig, J. Niessner, and I. Neuweiler, "Modeling gas-water processes in fractures with fracture flow properties obtained through upscaling," *Water Resources Research*, vol. 46, no. 9, Article ID W09528, pp. 201–210, 2010.

[6] T. Babadagli, X. Ren, and K. Develi, "Effects of fractal surface roughness and lithology on single and multiphase flow in a single fracture: an experimental investigation," *International Journal of Multiphase Flow*, vol. 68, pp. 40–58, 2015.

[7] A. Fumagalli and A. Scotti, "A numerical method for two-phase flow in fractured porous media with non-matching grids," *Advances in Water Resources*, vol. 62, pp. 454–464, 2013.

[8] V. L. Hauge and J. E. Aarnes, "Modeling of two-phase flow in fractured porous media on unstructured non-uniformly coarsened grids," *Transport in Porous Media*, vol. 77, no. 3, pp. 373–398, 2009.

[9] E. S. Romm, *Fluid Flow in fractured rocks*, Nebra Publishing House, Moscow, Russia, 1966.

[10] M. Fourar and R. Lenormand, "A viscous coupling model for relative permeabilities in a fracture," *Society of Petroleum Engineers Journal*, 1998.

[11] R. Brooks and A. Corey, *Hydraulic properties of porous media*, Colorado State University, 1964.

[12] J. R. Gilman and H. Kazemi, "Improvements in simulation of naturally fractured reservoirs," *Society of petroleum engineers Journal*, vol. 23, no. 4, pp. 695–707, 1983.

[13] L. K. Thomas, T. N. Dixon, and R. G. Pierson, "Fractured reservoir simulation," *Society of Petroleum Engineers Journal*, vol. 23, no. 1, pp. 42–54, 1983.

[14] S. Whitaker, "Flow in porous media II: The governing equations for immiscible, two-phase flow," *Transport in Porous Media*, vol. 1, no. 2, pp. 105–125, 1986.

[15] A. T. Corey, "The Interrelation between gas and oil relative permeabilities," *Producers Monthly*, vol. 19, p. 38, 1954.

[16] G. P. Diomampo, "Viscous Coupling in Two-phase flow in porous media and its effect on relative permeabilities," *Transport in Porous Media*, vol. 11, no. 3, pp. 201–218, 1993.

[17] M. Fourar and S. Bories, "Experimental study of air-water two-phase flow through a fracture (narrow channel)," *International Journal of Multiphase Flow*, vol. 21, no. 4, pp. 621–637, 1995.

[18] N. Watanabe, K. Sakurai, T. Ishibashi et al., "New v-type relative permeability curves for two-phase flows through subsurface fractures," *Water Resources Research*, vol. 51, no. 4, pp. 2807–2824, 2014.

[19] C.-Y. Chen, *Liquid-Gas Relative Permeabilities in Fractures: Effects of Flow Structures, Phase Transformation and Surface Roughness*, Stanford University, 2005.

[20] J. Reimann and W. Seeger, "Two-phase flow in a T-junction with a horizontal inlet. Part II: Pressure differences," *International Journal of Multiphase Flow*, vol. 12, no. 4, pp. 587–608, 1986.

[21] M. Fourar, S. Bories, R. Lenormand, and P. Persoff, "Two-phase flow in smooth and rough fractures: Measurement and correlation by porous-medium and pipe flow models," *Water Resources Research*, vol. 29, no. 11, pp. 3699–3708, 1993.

[22] A. Azzi, A. Al-Attiyah, Q. Liu, W. Cheema, and B. J. Azzopardi, "Gasliquid two-phase flow division at a micro-T-junction," *Chemical Engineering Science*, vol. 65, no. 13, pp. 3986–3993, 2010.

[23] S. Wang, K. He, and J. Huang, "Phase splitting of a slug-annular flow at a horizontal micro-T-junction," *International Journal of Heat and Mass Transfer*, vol. 54, no. 1-3, pp. 589–596, 2011.

[24] K. He, S. Wang, and J. Huang, "The effect of flow pattern on split of two-phase flow through a micro-T-junction," *International Journal of Heat and Mass Transfer*, vol. 54, no. 15-16, pp. 3587–3593, 2011.

[25] J. Chen, S. Wang, and S. Cheng, "Experimental investigation of two-phase distribution in parallel micro-T channels under adiabatic condition," *Chemical Engineering Science*, vol. 84, pp. 706–717, 2012.

[26] S. M. Bhagwat and A. J. Ghajar, "Experimental investigation of non-boiling gas-liquid two phase flow in downward inclined pipes," *Experimental Thermal and Fluid Science*, vol. 89, pp. 219–237, 2017.

[27] Y. Liu, W. Sun, W. Wu, and S. Wang, "Gas-liquid two-phase flow distribution in parallel micro-channels with different header and channels' orientations," *International Journal of Heat and Mass Transfer*, vol. 112, pp. 767–778, 2017.

[28] Y. Tabe, Y. Lee, T. Chikahisa, and M. Kozakai, "Numerical simulation of liquid water and gas flow in a channel and a simplified gas diffusion layer model of polymer electrolyte membrane fuel cells using the lattice Boltzmann method," *Journal of Power Sources*, vol. 193, no. 1, pp. 24–31, 2009.

[29] W. Seeger, J. Reimann, and U. Müller, "Two-phase flow in a T-junction with a horizontal inlet. Part I: Phase separation," *International Journal of Multiphase Flow*, vol. 12, no. 4, pp. 575–585, 1986.

[30] M. A. Mohamed, H. M. Soliman, and G. E. Sims, "Experimental investigation of two-phase flow splitting in an equal-sided impacting tee junction with inclined outlets," *Experimental Thermal and Fluid Science*, vol. 35, no. 6, pp. 1193–1201, 2011.

[31] H.-W. Li, J.-W. Li, Y.-L. Zhou et al., "Phase split characteristics of slug and annular flow in a dividing micro-T-junction," *Experimental Thermal and Fluid Science*, vol. 80, pp. 244–258, 2017.

[32] S. Kim and S. Y. Lee, "Split of two-phase plug flow with elongated bubbles at a microscale branching T-junction," *Chemical Engineering Science*, vol. 134, pp. 119–128, 2015.

[33] J. Chen, S. Wang, H. Ke, S. Cai, and Y. Zhao, "Gas-liquid two-phase flow splitting at microchannel junctions with different branch angles," *Chemical Engineering Science*, vol. 104, pp. 881–890, 2013.

[34] W. Sun, Y. Liu, K. He, and S. Wang, "The phase distribution of gas-liquid two-phase flow in microimpacting T-junctions with different branch channel diameters," *Chemical Engineering Journal*, vol. 333, pp. 34–42, 2018.

[35] G. Radilla, A. Nowamooz, and M. Fourar, "Modeling non-Darcian single- and two-phase flow in transparent replicas of rough-walled rock fractures," *Transport in Porous Media*, vol. 98, no. 2, pp. 401–426, 2013.

[36] M. Fourar and R. Lenormand, "Inertial effects in two-phase flow through fractures," *Oil & Gas Science and Technology*, vol. 55, no. 3, pp. 259–268, 2000.

[37] B. Li, R. Liu, and Y. Jiang, "Influences of hydraulic gradient, surface roughness, intersecting angle, and scale effect on nonlinear flow behavior at single fracture intersections," *Journal of Hydrology*, vol. 538, pp. 440–453, 2016.